Boletín de la Sociedad Geológica del Perú

Journal homepage: www.sgp.org.pe

Using Stable Isotopes to better understand the Petrologic and Hydrothermal Evolution of Cretaceous Linga Complex of the Peruvian Coastal Batholith, near Ica

González Olivares, Luciano U. [1], Clausen, Benjamin L[2], Holk, Gregory J[3], Poma, Orlando[4]

ABSTRACT

Oxygen and hydrogen isotope values obtained from 64 minerals separated from 18 samples are employed to determine the source of magma and hydrothermal fluids that caused potassic, propylitic, phyllic, and argillic alteration in the Linga complex, situated near Ica in the mid-to-late Cretaceous 96-97 M.a Peruvian Coastal Batholith (Moore 1984 & Beckinsale 1985).

Calculated $\delta^{18}O$ plagioclase values in fresh samples are between +6.7‰ and +7.9‰ at equilibrium with $^{18}O/^{16}O$ crystallization temperatures between 588°C and 654°C. A slight west-to-east and older-to-younger increasing trend in $\delta^{18}O$ values for fresh samples suggests a slightly greater crustal component to the east. Pervasive potassic and propylitic alteration assemblages yielded average values for $\delta^{18}O$ of +7‰ and for δD of –50‰ suggesting that alteration was primarily caused by magmatic fluids; however, other fluids were also involved. High plagioclase (+9.3‰) and hornblende (+6.3‰) $\delta^{18}O$ values from one sample near a pluton contact suggest interaction with metamorphic or low temperature fluids. High epidote δD values from altered diorite (–25.8‰) and monzonite (–36.1‰) suggest seawater infiltration west of the batholith. The average water/rock ratio of 0.1 suggests 1 part of external meteoric or metamorphic fluids to 10 parts rock or magmatic fluids, indicating the significant role of magmatic hydrothermal fluids in the alteration.

RESUMEN

Los valores isotópicos de oxígeno e hidrógeno de 64 minerales aislados de 18 muestras se usaron para conocer el origen de los fluidos hidrotermales que causaron alteración potásica, propilítica, fílica y argílica en el complejo Linga cerca de Ica del Batolito Costero Peruano del Cretáceo medio-superior 96-97 M.a (Moore 1984 & Beckinsale 1985).

Valores de $\delta^{18}O$ plagioclasa, en roca fresca, varían de +6,7‰ a +7,9‰ en equilibrio con temperaturas de cristalización de $^{18}O/^{16}O$ entre 588°C a 654°C. El leve incremento de oeste-este de más antiguos-recientes en valores $\delta^{18}O$ de muestras frescas sugiere un componente cortical ligeramente mayor hacia el este. Ensambles de alteración pervasiva potásica y propilítica dieron valores promedio de + 7‰ en $\delta^{18}O$ y -50‰ en δD, sugiriendo principalmente alteración por fluidos magmáticos. Sin embargo, otros fluidos también se involucraron. Altos valores de $\delta^{18}O$ (+9.3‰) plagioclasa y $\delta^{18}O$ (+6.3‰) hornblenda de una muestra cerca de un contacto plutónico, sugieren interacción con fluidos metamórficos o fluidos de baja temperatura. Altos valores en δD epidota (–25.8‰) de diorita alterada y de monzonita (–36.1‰), sugieren infiltración de agua marina al oeste del batolito. El valor promedio de 1/10 en la ratio agua/roca indica una parte de agua meteórica externa o fluidos metamórficos por 10 partes de fluidos magmáticos, indicando alteración principalmente por el rol de fluidos magmáticos hidrotermales en la alteración.

Palabras claves: *Stable Isotopes, isotopic equilibrium, hydrothermal alteration, hydrothermal fluids, Peru, Cretaceous*

[1] *Universidad de Montemorelos, Montemorelos N. León, Méx. (lugo@um.edu.mx)*

[2] *Geoscience Research Institute & Department of Earth and Biological Sciences, Loma Linda University, Loma Linda CA, USA. (bclausen@llu.edu)*

[3] *California State University, Long Beach, Department of Geological Sciences and the Institute for Integrated Research in Materials, Environments and Societies, Long Beach CA, USA (gregory.holk@csulb.edu)*

[4] *Universidad Peruana Unión, Ñaña, Peru*

1. INTRODUCCIÓN

Earth, with its hydrosphere, active lithosphere and upper mantle, has an enormous potential to trigger a variety of interactions between aqueous fluids and rocks. Oxygen and hydrogen isotopes are valuable for understanding these interactions because they can help identify fluid sources, pathways and flux estimates (Brandriss et al., 1995; Sharp, 2007; Taylor, 1978). Stable isotope studies of numerous igneous rock suites have dramatically transformed our perspective on the role of such fluids in the evolution of the crust (e.g., Gregory and Criss, 1986).

Magma experiences numerous changes in composition during transport from its source to the site of emplacement or eruption (Rutherford and Devine, 2003; Sykes, 1987). In particular, changes in stable isotopic composition occur as magmas are affected by partial melting (Williams et al., 2009), contamination (Garcia et al., 2008; Harris and Chaumba, 2001; Santo and Peccerillo, 2008), magma mixing (Bindeman, 2008; Johnson et al., 1996), fractional crystallization (DePaolo, 1981; Sparks and Huppert, 1984), degassing (Taylor, 1986), and hydrothermal alteration (Dilles et al., 1992; Grunder, 1992; Harris and Golding, 2002).

Stable isotope studies have shown that subsolidus hydrothermal processes that affect plutons emplaced near Earth's surface are the result of water from different sources that include magmatic (Giachetti et al., 2015; Plank et al., 2013), metamorphic (Barnes, 1970; Yardley and Cleverley, 2013), oceanic (German and Lin, 2004; Humphris, 1976; Rohling, 2013), connate (Husband, 1998), and meteoric waters (Bowen and Revenaugh, 2003; Brandriss et al., 1995; Terzer et al., 2013). All can serve as ore-forming fluids (Guilbert and Park, 1986; Hedenquist and Lowenstern, 1994; Jebrak, 1997; Robb, 2005). Other components in these solutions, such as dissolved ions and gasses, yield significant additional information about the pressure-temperature evolution of the solution and the fluid pH and oxidation state (Markl and Baumgartner, 2002; Rose and Burt, 1979; Taylor, 1986). Lithologies with which the fluid has interacted along its flow path influence these variables through alteration reactions (Mysen, 2014; Seyfried et al., 1988).

The origin of magmas and hydrothermal fluids at the Linga complex in the northern Arequipa segment of the Cretaceous Peruvian Coastal Batholith near Ica, is investigated using stable isotopes from fresh rocks and the various alteration facies recorded in them. Mineral $\delta^{18}O$ and δD values from unaltered rocks yield insight into magma sources and how they differ with location, age, composition, and apparent temperature. Style and temperatures of alteration and the areal extent of alteration are identified in the field and in thin section. Hydrothermal fluid sources and water/rock ratios are indicated by $\delta^{18}O$ and δD values from these altered rocks.

2. GEOLOGIC SETTING

2.1. The Peruvian Coastal Batholith (PCB)

The Andes Cordillera is the largest and longest-lived active subduction-related orogeny on Earth (Schilling et al., 2006; Springer, 1999). It results from subduction of the oceanic Farallon Plate and later the Nazca Plate under the continental crust of the South American Plate beginning in the Cretaceous (Martinod et al., 2010; Pfiffner and Gonzalez, 2013; Polliand et al., 2005).

Convergence rates between these two plates increased dramatically during the late Early to Late Cretaceous and shifted to having a significant oblique component (Jaillard and Soler, 1996; McQuarrie et al., 2005; Mégard, 1984); this resulted in a trenchward motion of the South American plate, subduction erosion (Jaillard and Soler, 1996; Polliand et al., 2005), significant arc magmatism, and the emergence of volcano-sedimentary basins of the Mesozoic Western Peruvian Trough (Mégard, 1984; Pfiffner and Gonzalez, 2013). The development of this trough was followed by the intrusion of magmas between about 100 Ma and 30 Ma ago that yielded the numerous plutonic suites that comprise the Peruvian Coastal Batholith (PCB) shown in Figure 1 (Polliand et al., 2005; Soler and Bonhomme, 1990).

The PCB has a geometry and composite nature similar to other circum-Pacific batholiths, but is one of the largest. In addition, the PCB has preserved its integrity unlike the batholiths of western North America which have been partially disarticulated by later tectonic events, obscuring their relationships with the plate margin at the time of emplacement (Atwater, 1970; Schweickert and Cowan, 1975; Winter, 2010).

The abundant intrusions that comprise the Mesozoic-Cenozoic PCB constitute an exceptional example of long-lived plutonism related to a convergent margin. This batholith, parallel to the contemporary Peru-Chile trench along almost its entire 2000 km length, displays significant longitudinal differences in magma type and emplacement history, dividing into five segments. From north to south these segments are termed Piura, Trujillo, Lima, Arequipa, and Toquepala (Figure 1). Each segment is characterized by its own particular suite of intrusions which can be grouped into Super-units, and each Super-unit comprises a set of units closely related in space, time, chemistry, and petrology (Cobbing and Pitcher, 1972; Cobbing et al., 1977; Moore, 1984).

The 900 km-long Arequipa segment, the longest of the PCB, extends from the Lurín District in the Lima Province southeast to Arequipa. This segment has been broadly mapped, with some of the most thorough mapping in the Rio Pisco and Rio Ica areas, providing detailed documentation of emplacement and petrologic processes (Agar, 1978; Cobbing et al., 1977; Moore, 1979).

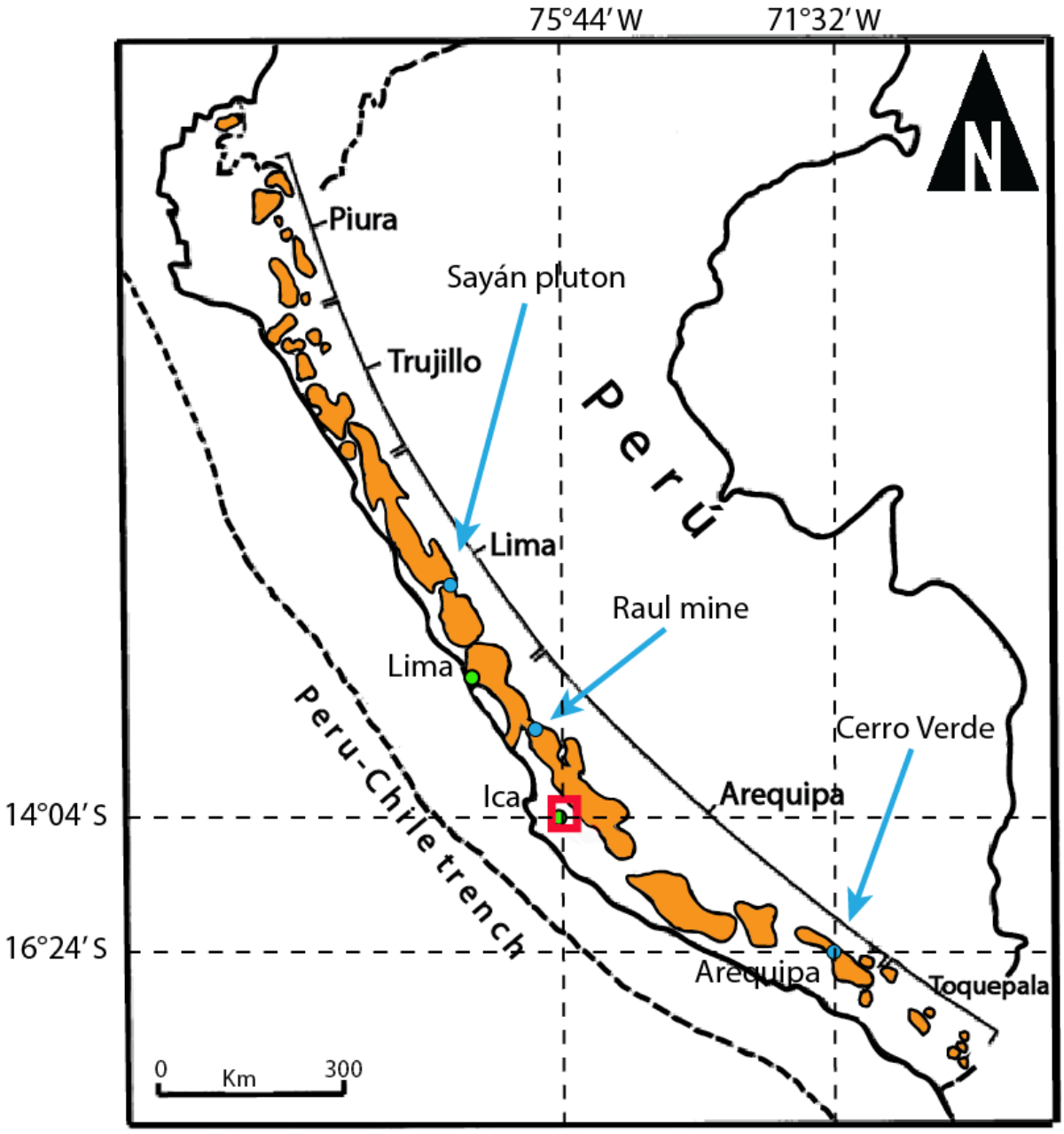

Figure 1. The five segments of the Peruvian Coastal Batholith with the location of previous stable isotope studies indicated in blue and the study area in red. Adapted from Moore (1984).

2.2. Brief description of rock units in the Ica-Pisco section of the PCB

Rock units mapped in the Rio Ica and Rio Pisco section of the Arequipa segment of the PCB are shown in Figure 2. The Quilmana and Yura are Pre-PCB volcanic-sedimentary units primarily to the west and east of the PCB respectively. Early magmatic activity related to the PCB consists of gabbros. Then the Linga, Pampahuasi, Tiabaya, and Incahuasi Super-units form the main granitic units of the PCB.

Of the two major Pre-PCB volcanic-sedimentary units, the Yura group on the east is older. It has a thickness of 2000 m in the Rio Ica and up to 600 m of quartzite with interbedded shales northeast in the Rio Pisco (Moore, 1979). The Yura group in the eastern Rio Pisco area also includes volcanics (porphyritic andesites). The age of the Yura group is constrained to between 216 Ma and 134 Ma (Boekhout et al., 2013, see Alvan et al.,). The Quilmana volcanics, whose maximum emplacement age is about 113 Ma (Moore, 1979; Mukasa, 1986), dates back to the emergence of the Western Peruvian Trough (Aguirre and Offler, 1985). This unit includes the younger stratified rocks cut by the PCB and constitute a large part of its western and eastern envelope. The main lithology is metamorphic hornfels and the most abundant alteration minerals are biotite and epidote (Moore, 1979).

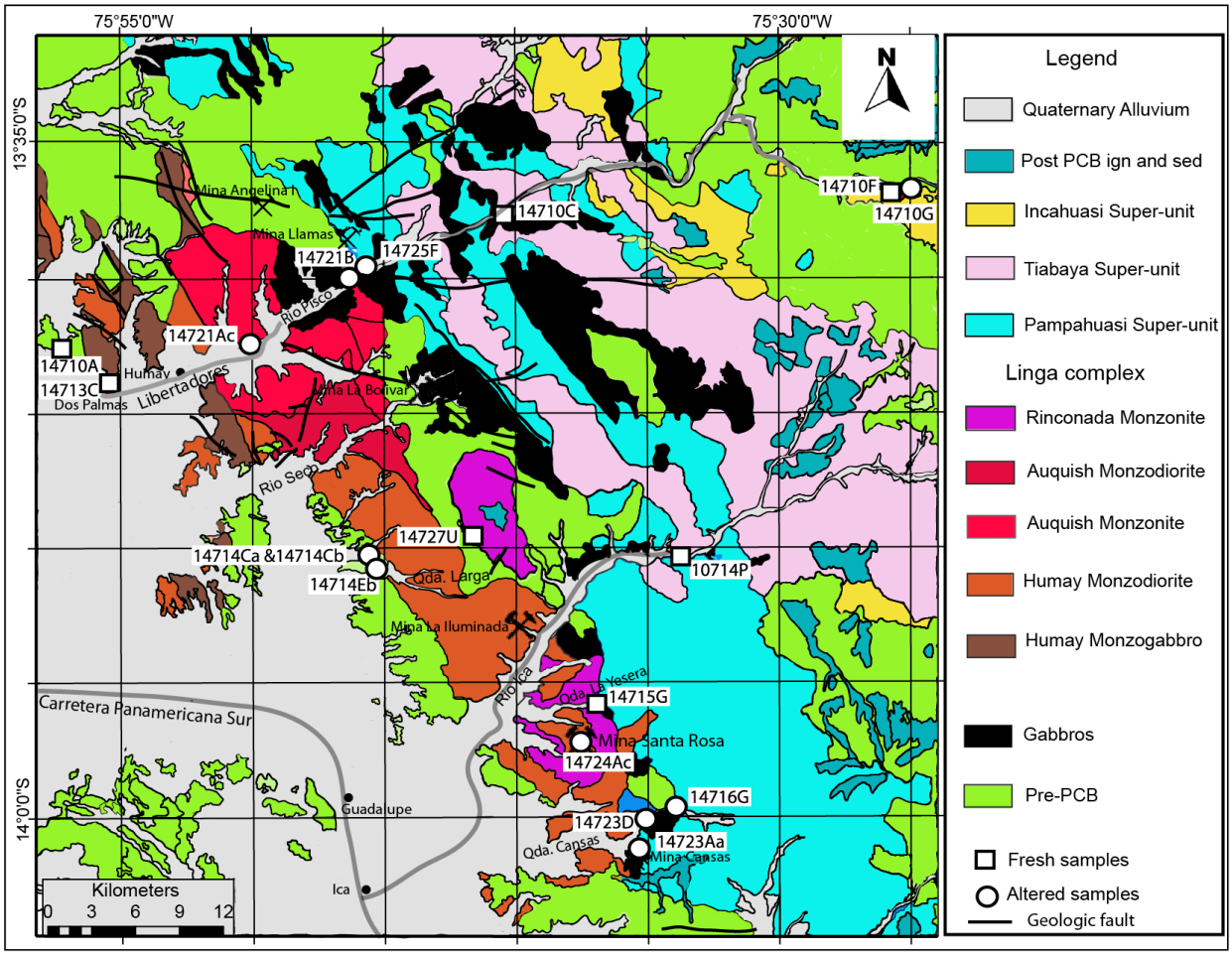

Figure 2. Simplified geologic map of the Ica-Pisco area in the Peruvian Costal Batholith. Sample locations and Super-units are indicated. The map includes the quadrangle 28-i (Guadalupe) and parts of quadrangles 28-m (Santiago de Chocorvos), 29-m (Cordova) and 29-i (Ica). Adapted from Instituto Geológico, Minero y Metalúrgico del Perú (INGEMMET, 1978).

Gabbros that have been interpreted to correspond to the Patap gabbros in the Lima segment (Mukasa, 1986) are minor plutons broadly spread over a large part of the Arequipa segment. Previously the age of gabbroic plutons in the Ica-Pisco area has been bracketed between the 113 Ma Aptian/Albian boundary as the maximum emplacement age of the Quilmana volcaniclastics, which they intrude, and the 101.4 Ma concordant zircon crystallization ages of the oldest granitoids that cut the gabbros (Moore, 1979; Mukasa, 1986). However, Martinez (2016) found an age of 131 Ma for these gabbros and suggested that gabbros with younger ages may be cumulates of the PCB granitoids.

The Linga complex, the focus of this paper, is at the western margin of the PCB. This unit ranges from monzogabbro to monzogranite composition. In the monzogabbros and monzodiorites, cumulose textures are well preserved whereas granophyric textures, which suggests rapid cooling at shallow depths, prevail in the monzogranitic units (Agar, 1981; Mukasa, 1986). This consanguineous suite of intrusive rocks is interpreted to have originated from magmatic differentiation of a single parent magma (Agar, 1978) and is divided into three units: the Humay, Auquish and Rinconada (Agar, 1981).
The earliest Humay unit is the most mafic and is comprised of quartz monzodiorite, quartz monzogabbro and monzogabbro. Mafics are present as small clots and subhedral prisms of hornblende as well as small flecks of biotite. This elongate unit is exposed along the western edge of the Linga complex and follows the Andean trend. Martinez (2016) determined no age for this unit, but inferred that it must be older than the 105 Ma Auquish unit which it intrudes. One of the main differences between the Humay Monzogabbro and the Humay Monzodiorite units is their K_2O content, 1.2% for the former and 2.4% or the latter (Agar, 1981).

The 105-103 Ma (Martinez, 2016) Auquish unit is mostly porphyritic monzogranites and quartz monzodiorite. Mineralogy consists of hornblende, orthoclase and quartz, as well as varying proportions of accessory minerals. This unit is located northeast of the Humay unit and has a geometry like a ring complex. The Auquish monzodiorite unit belongs to a group of nested arcuate plutons and is particularly xenolithic immediately below its roof (Agar and Le Bel, 1985). The Auquish monzonite unit is characterized by relatively straight local schlieren layering and abundant mafic enclaves at its contacts with the Humay unit (Martinez, 2016).
The 100-96 Ma (Martinez, 2016) Rinconada unit is mostly monzogranite, characterized by grey-pink feldspar, pale plagioclase and quartz as well as small prisms of hornblende and sparse biotite. This unit outcrops in the

southern part of the Linga complex and has an elliptical spatial distribution (Agar and Le Bel, 1985; Moore, 1979). Large elongate and steep-walled plutons of the 98-90 Ma (Martinez, 2016) Pampahuasi Super-unit in the Arequipa segment are characterized by diorite and tonalite with well-developed mineral fabrics and localized shear banding (Moore, 1979; Mukasa, 1986). Plagioclase is coarse-grained and euhedral, and hornblende is present with poikilitic biotite.

The 87-82 Ma (Martinez, 2016) Tiabaya Super-unit is distinguished by hornblende and biotite occurring as euhedral grains and plagioclase appearing as crystals up to 1 cm long. The lithology is made up of tonalite, granodiorite and quartz monzonite. This unit occurs extensively throughout the Arequipa segment (Agar, 1978).

The 69-58 Ma (Martinez, 2016) Incahuasi Super-unit is characterized by pervasive poikilitic hornblende and biotite in a framework of euhedral plagioclase. Its main lithology is quartz diorite to monzogranite (Agar, 1978).

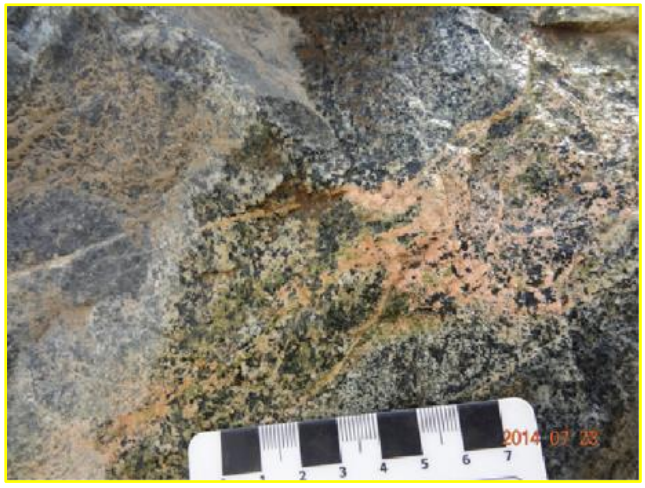

3. PREVIOUS STABLE ISOTOPE STUDIES IN THE PCB

Few stable isotope data exist for the PCB. Beckinsale et al. (1985) report whole rock $\delta^{18}O$ values between +6.3‰ and +8.6‰ (n = 11) for fresh samples from the Sayán pluton (Figure 1) 150 km north of Lima in the Lima segment. These data are interpreted to be the product of fractional crystallization (Taylor, 1978).

More data exist for portions of the PCB that have been affected by hydrothermal systems related to mineralization. Phengite δD values of – 67‰ to – 47‰ and calcite $\delta^{18}O$ values of +15‰ to +30‰ (Le Bel, 1985) suggest a magmatic origin for alteration fluids at the Cerro Verde porphyry Cu deposit near Arequipa (Figure 1); however, high calcite $\delta^{18}O$ values at high structural levels suggest the involvement of meteoric hydrothermal fluids at low temperatures (< 100°C).

Another study was done at the Raul mine, a complex metamorphosed strata-bound vein-rich sulphur deposit (De Haller et al., 2006; Ripley and Ohmoto, 1979) 150 km south of Lima (Figure 1). It revealed amphibole δD values of –60‰ to –21‰ (n = 15), whole rock $\delta^{18}O$ values of +7.8‰ to +10.8‰ (n = 11), and vein calcite $\delta^{18}O$ values of +14.0‰ to +14.2‰ (n = 2). These data suggest the involvement of seawater modified by evaporation and/or shale membrane processes during mineralization (Ripley and Ohmoto, 1979).

Figure 3. a) Outcrop at the Pampahuasi-Humay boundary with abundant K-feldspar, biotite and magnetite indicating potassic alteration probably at temperatures of 450 to 600°C.

Figure 3. b) Outcrop at the Pampahuasi-Humay boundary with widespread epidote indicating propylitic alteration probably at temperatures of 250 to 350°C. Both outcrops are in the Rio Cansas transect.

4. HYDROTHERMAL ALTERATION IN THE LINGA COMPLEX

Potassic, propylitic, and sericitic alteration are common in units of the Linga complex. The alteration patterns are frequently organized concentrically in areas surrounding the intrusion with the potassic alteration in the center and the propylitic alteration toward the edge of the pluton (Agar, 1981).

Potassic alteration (Figure 3a) results from potassium enrichment. It is particularly abundant and important in porphyry and epithermal mineralizing systems where it occurs in the high temperature core zones.

Potassium silicate alteration results from the replacement of plagioclase and mafic silicate minerals with K-feldspar and secondary biotite/sericite (Figure 4a) at temperatures of 450°C to 600°C (Pirajno, 2009). This type of alteration can occur before complete crystallization of magma (Damian, 2003; Rose and Burt, 1979).

Propylitic alteration (Figure 3b) is characterized by the addition of H_2O and CO_2 with no substantial acidic metasomatism. It becomes more pervasive close to the heat and fluid source of a hydrothermal deposit (Pirajno, 2009) and normally forms at 250°C to 350°C (Dilles et al., 1992; Hedenquist et al., 2000). Characteristic mineral assemblages of propylitic alteration are albite, chlorite, epidote, carbonates, sericite, pyrite and magnetite (Figure 4b), mostly replacing plagioclase (Rose and Burt, 1979).

Phyllic alteration is common in granitic intrusions related to porphyry copper and other vein-alteration ore deposits (Que and Allen, 1996). Both potassium feldspar and plagioclase are converted to sericite and minor amounts of clay minerals (Figure 4c) (Rose and Burt, 1979). Sericitization in the phyllic facies generally occurs between 200° and 350°C (Hedenquist et al., 2000; Meunier and Velde, 2004).

Argillic alteration (Figure 4d) results from the total conversion of feldspar and amphiboles to the low temperature (< 200°C) minerals (Meunier and Velde, 2004) dickite, kaolinite, and montmorillonite, along with sericite and other clay minerals. This style of alteration is related to leaching of calcium, sodium and magnesium by acidic fluids (Pirajno, 2009; Rose and Burt, 1979).

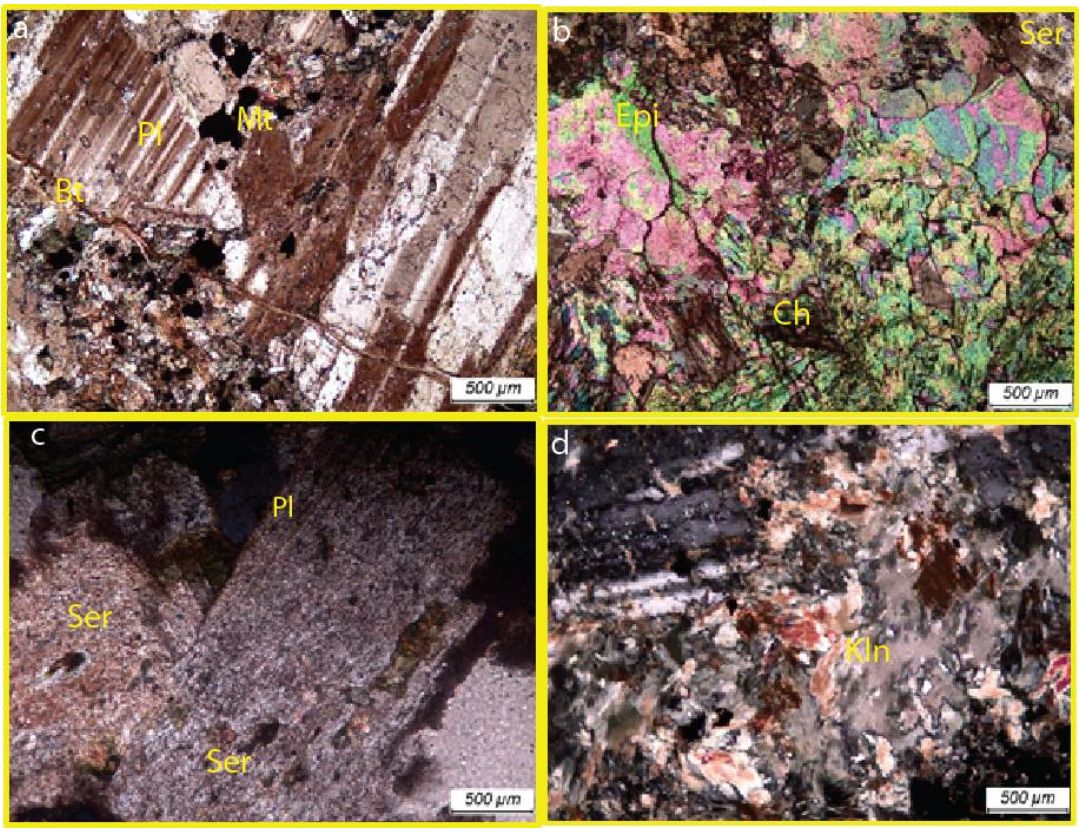

Figure 4. Thin sections (with crossed-polars) of four types of alteration mentioned in the text and observed in the Linga complex. a) Potassic alteration in sample 14714Ca from the border between Humay and the volcanics in the Quebrada Larga transect. Note the secondary biotite (Bt) veinlets cutting plagioclase (Pl) crystals and the groundmass and magnetite (Mt). b) Propylitic alteration in sample 14723D from the border between Humay and Pampahuasi. Note the abundance of epidote (Epi) and chlorite (Ch). c) Phyllic alteration in sample 13828A in the Rio Pisco transect with sericite (Ser) replacing plagioclase (Pl). d) Argillic alteration in sample 14714Cb from the border between Humay and the volcanics in the Quebrada Larga transect with a clay mineral, probably kaolinite (Kln), replacing plagioclase.

5. ANALYTICAL TECHNIQUES

Most samples were collected along southwest to northeast trending rivers that cut the Linga complex in the Ica-Pisco area. Transects include the Quebrada Cansas, Rio Ica, Quebrada Larga, and Rio Pisco (Figure 2) with focus on contact zones between Super-units to identify styles of hydrothermal alteration. Published geologic maps of the Guadalupe and Ica quadrangles (INGEMMET, 1978) guided these efforts. Rock samples selected for isotopic analysis are representative of the Super-units in this part of the PCB. Petrographic analysis identified the style of alteration and minerals available for isotope analysis. Minerals were separated from 18 samples by Yu-Neng Mineral Separation Co. Langfang, China.

All stable isotope measurements were performed using the ThermoFinnigan DeltaPlusXP mass spectrometer at the Institute for Integrated Research in Materials, Environments and Societies at California State University, Long Beach. Oxygen was extracted from silicate minerals using a modified version of the laser fluorination method (Sharp, 1990). Oxygen isotope values are reported relative to V-SMOW, where NBS-28 has $\delta^{18}O$ = +9.6‰ on this scale. Replicate analyses of Caltech rose quartz working standard ($\delta^{18}O$ = +8.45‰) have an analytical error of ±0.2‰. Hydrogen was liberated from biotite, amphibole and epidote using the carbon reduction technique described by Sharp et al. (2001). Hydrogen isotope data are reported relative to V-SMOW. Multiples analyses of NBS-30 biotite standard (δD = −65.7‰) indicates an analytical error of ±2.0‰. Water content of minerals analyzed for hydrogen isotopes was determined by comparing the area under the gas chromatograph peak for mass 2 to a calibration of area versus sample size for NBS-30 biotite (3.5‰ H_2O). Quality control and reproducibility is shown by duplicate measurements on 20% of samples analyzed for oxygen isotopes and all samples analyzed for hydrogen isotopes.

6. RESULTS

Table 1 shows 48 $\delta^{18}O$ values and 16 δD values acquired from 18 samples from the Ica-Pisco section of the PCB.

Seven samples are fresh and eleven are altered. This table also shows four estimated $\delta^{18}O$ values for plagioclase. Sample locations are indicated in Figure 2.

6.1 *Unaltered intrusive rocks*

The $\delta^{18}O$ values in Table 1 are from rocks that belong to each of the Super-units with the range of values for each mineral from unaltered rocks being: quartz (+9.1 to +9.8‰, n = 4), K-feldspar (+7.4 to +8.2‰, n = 3), plagioclase (+6.7 to +7.9‰, n = 7), hornblende (+5.5 to +6.2‰, n = 5), and biotite (+3.9 to 5.5‰, n = 4). The values are consistent with a continental magmatic arc origin (Taylor and Sheppard, 1986). Likewise, biotite (–80.8 to –74.5‰, n = 4) and hornblende (–86.7 to –63.9‰, n = 5) δD values are primary magmatic values.

6.1.1 *Primary magma sources*

Plagioclase $\delta^{18}O$ values from unaltered rocks increase from approximately +7‰ to +8‰ in a west-to-east direction (Figure 5). The same data is displayed in Figure 6 by decreasing age from approximately +7‰ at 130 Ma to +8‰ at 70 Ma.

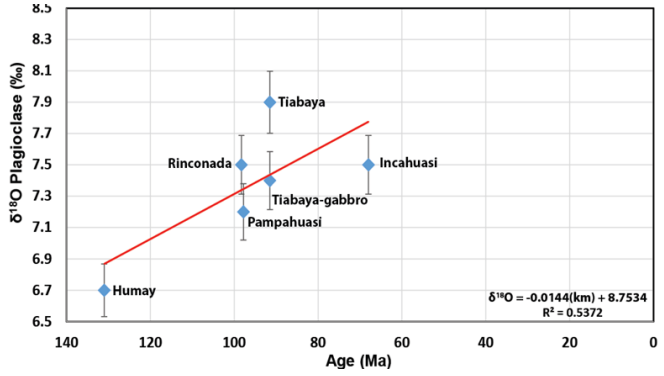

Figure 5. Values of $\delta^{18}O$ for fresh samples ordered from west to east. Note the slight increasing trend resembling that in the Peninsular Ranges Batholith of California (Clausen et al., 2014; Schmidt and Paterson, 2002; Silver et al., 1979). The error bars are ±0.2‰. Errors come from the California State University Long Beach CSULB isotope laboratory.

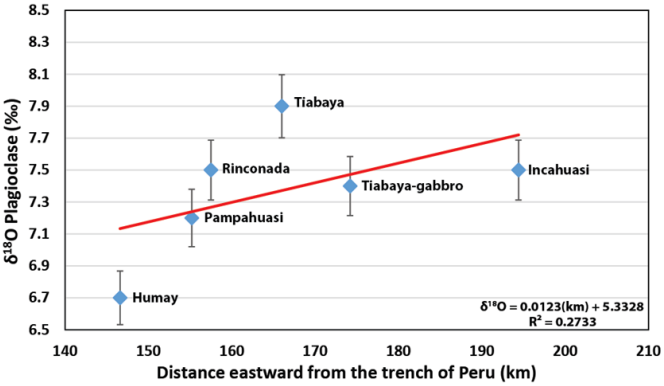

Figure 6. Values of $\delta^{18}O$ for fresh samples ordered from older to younger. Note the slight increasing trend as the rocks become younger, which corresponds to the west-to-east trend shown in Figure 5. The error bars are ±0.2‰. Errors come from the CSULB isotope laboratory.

Table 1. Oxygen and hydrogen isotope values in units of per mil for fresh and altered (*) samples. Blue colored values were estimated based on the δ18O values of other minerals in the same mineralization assemblage (Bottinga and Javoy, 1975). Quartz (Qtz), K-feldspar (Kfs), plagioclase (Pl), hornblende (Hbl), actinolite (Act), Biotite (Bt), epidote (Epi), and magnetite (Mt).

Unit	Sample	δD values				$\delta^{18}O$ values							
		Bt	Hbl	Epi	Act	Mt	Epi	Act	Bt	Hbl	Pl	Kfs	Qtz
Incahuasi													
	14710F	-78.2	-74.9						3.9	6.2	7.5	8.2	9.1
Tiabaya													
	10714P	-80.8	-76.4						5.5	5.9	7.9	8.2	9.8
Pampahuasi													
	14723Aa*										8.4		8.9
	14725F*		-89.2							3.6	*6.9*		8.9
	14715G	-74.5	-73.7						5.4	5.5	7.2		9.1
	14723D*			-25.6	-78.6		3.5	4.2			*6.8*		
	14716G*		-83.7							6.3	9.3		
Linga-Rinconada													
	14727U	-80.6	-86.7			1.5			4.6	5.8	7.5	7.4	9.2
	14724Ac*	-73.8							3.3		5.7		7.3
Linga-Auquish													
	14721Ac*					0.5					*5.5*	5.6	5.5
	14721B*			-36.1			3.2				*7.1*		
Linga-Humay													
	14714Eb*										8.2	8.5	8.2
	14714Ca*										7.6	7.6	
	14713C					1.6					6.7		
Gabbro													
	14710C		-63.9							5.7	7.4		
Quilmana (Pre-PCB)													
	14714Cb*										7.4		
	14710A										7.6		
Yura Group (Pre-PCB)													
	14710G*	-86.5							0.1		2.6		

These increasing values indicate the incorporation of more crustal material from west to east and with time. Since the range in $\delta^{18}O$ values is so small, error bars of ±0.2‰ are included in Figures 5 and 6.

The west-east increase of +6.7 to +7.9‰ is smaller than the range observed for whole rock $\delta^{18}O$ values from the Peninsular Ranges Batholith (+6‰ to +12‰, Silver et al., 1979). Contaminated mantle melts display a rise in $\delta^{18}O$ values in correlation with increasing SiO_2 (Hoefs, 1996). The trend of $\delta^{18}O$ in the Peninsular Ranges Batholith indicates a mantle magma source in the west contaminated by an ^{18}O source increasing eastward. In contrast, our data indicate only slight contamination of primary magma from a mantle source for the PCB in the Ica-Pisco area. This is consistent with a restricted range of depleted mantle initial $^{87}Sr/^{86}Sr$ (Sr_i) values (0.7036-0.7065) observed in Ica-Pisco area (Martinez et al., 2016) with slight increases of Sr_i toward the northeast.

Near Arequipa, magmas related to the Arequipa segment intruded Precambrian cratonal rocks of the Arequipa massif, as well as Pre-PCB volcanic and sedimentary units. Increased contamination of crustal material is reflected by a much larger range of initial $^{87}Sr/^{86}Sr$ ratios from 0.7036 to 0.7084 (Beckinsale et al., 1985) and a slightly higher $\delta^{18}O$ value of +9‰ (Le Bel, 1985) from a pluton related to the Cerro Verde porphyry Cu deposit. For comparison, this range of Sr_i values are similar to those from the Peninsular Ranges Batholith of 0.703 to 0.709 (Langenheim et al., 2004; Silver et al., 1979), another batholith displaying an eastward increasing crustal

component as magmatism shifted in that direction due to shallowing subduction. This trend is not as pronounced in the Peruvian batholith.

6.1.2 *A test of $^{18}O/^{16}O$ equilibrium and geothermometry for unaltered rocks*

Closure temperatures can be estimated using $\delta^{18}O$ values measured for all major minerals that comprise an intrusive rock along with the employment of $^{18}O/^{16}O$ fractionation factors between quartz and each mineral (Bottinga and Javoy, 1975; Faure and Mensing, 2009). The temperature dependence of the isotopic fractionation factors of oxygen and oxide minerals are given by equations (Bottinga and Javoy, 1975) with the form

$$10^3 ln\, \alpha_b^a = A + \frac{B \times 10^6}{T^2} \qquad (1)$$

where α is the isotopic fractionation factor between two coexisting minerals a and b, T is the temperature in Kelvins, and A and B are experimentally determined constants. Equation (1) is linear at temperatures > 300°C (Sharp, 2007) when plotted with $10^6/T^2$ as the x-axis and can be expressed as

$$\delta_a - \delta_b = \Delta_b^a = 10^3 ln\, \alpha_b^a = A + \frac{B \times 10^6}{T^2}, \qquad (2)$$

where $\delta_a - \delta_b = \Delta_b^a$ applies at temperatures > 300°C (Gregory et al., 1989). By designating quartz as mineral a, the B coefficient (Table 2) for each other mineral (b) is used to calculate equilibrium temperatures. If a and b are non-hydrous minerals, then A = 0.

However, if the minerals such as amphibole and biotite contain hydroxyl groups, then the A value is –0.3 and –0.6 respectively (Javoy, 1977). Equation (2) is useful in that the difference $\delta_a - \delta_b$ between various pairs of minerals can be used to determine the equilibrium temperature of the coexisting minerals (Bindeman, 2008; Javoy et al., 1970; Turi, 1988).

The resulting equilibrium temperature is equal or less than the temperature of crystallization, since the minerals may have continued exchanging oxygen isotopes while the rock was cooling after crystallization (Giletti and Hess, 1988). The oxygen isotope temperature is valid under the assumption that minerals are in equilibrium when isotope exchange ceased and that the mineral assemblage was not disturbed by interaction with sub-solidus external aqueous fluids (Faure and Mensing, 2009; Guilbert and Park, 1986).

Oxygen isotopic equilibrium can be tested graphically with the "isotherm method" of (Javoy et al., 1970) that uses the experimentally and theoretically determined A and B parameters of equation (2). According to this method, individual minerals from a rock that are in isotopic equilibrium fall on a straight line that crosses the zero-zero point (representing quartz), and whose slope $10^6/T^2$, yields apparent equilibrium temperature.

This "isotherm method" yields better results if the number of mineral $\delta^{18}O$ values is maximized and cover as large a range of $\delta^{18}O$ values as possible, such as covering the range between quartz and magnetite (Holk et al., 2016).

The application of this method to unaltered samples reveals apparent isotopic equilibrium at temperatures between 588° and 654°C (Figure 7).

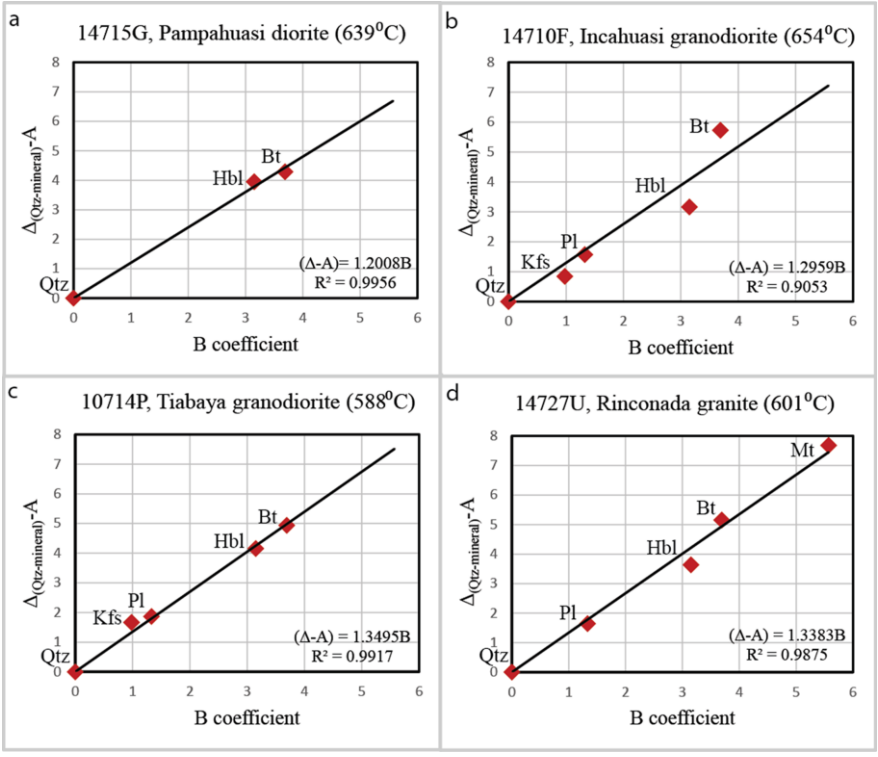

Figure 7. Thermometry plots for four fresh samples from the Linga complex. Values of R2 greater than 0.9 indicate isotopic equilibrium between minerals. Temperatures were obtained using equation (2) in the text. Quartz (Qtz), K-feldspar (Kfs), plagioclase (Pl), hornblende (Hbl), biotite (Bt), magnetite (Mt).

The highest equilibrium temperatures are from the Incahuasi granodiorite (654^{0}C) and Pampahuasi diorite (639°C), but the latter result is from only three minerals. The Tiabaya granodiorite and the Linga Rinconada granite showed an apparent isotopic equilibrium at lower temperatures of 588 and 601^{0}C, respectively.

6.2 *Altered samples*

Samples that display evidence for alteration in both the field and thin section have mineral $\delta^{18}O$ values (Table 1) out of equilibrium, including quartz (+8.9‰), K-feldspar (+5.6 to +8.5‰, n = 3), plagioclase (+2.6 to +9.3, n = 11), hornblende (+3.6 to +6.3‰, n = 2), biotite (+0.1 to +3.3‰, n = 2), actinolite (+4.2‰), epidote (+3.2 to 3.5‰, n = 2), and magnetite (+0.5‰), that suggest interaction with external fluids of various types. This is supported by δD values from biotite (–86.5 to –73.8‰, n = 2), hornblende (–89.2 to –83.7‰, n = 2), actinolite (–78.6‰), and epidote (–36.1 to –25.6‰, n = 2).

6.2.1 *Identification of fluid sources using isotope data based on altered samples*

Stable isotope values from mineral and mineral-H_2O fractionation factors can be used to identify the source of the hydrothermal fluids responsible for these sub-solidus mineralogical changes in the rock, if the alteration temperature is known. Such fluids (Figure 8) include seawater ($\delta^{18}O$ and δD~ 0‰; Faure, 1998; Rollinson, 1993), magmatic water ($\delta^{18}O$ = +6 to +10‰, δD = –80 to –40‰; Sheppard, 1986), metamorphic waters ($\delta^{18}O$ = +3 to +25‰, δD = –65 to –20‰; Guilbert and Park, 1986; Rollinson, 1993), and meteoric-hydrothermal water with variably low $\delta^{18}O$ and δD values (Sheppard, 1986).

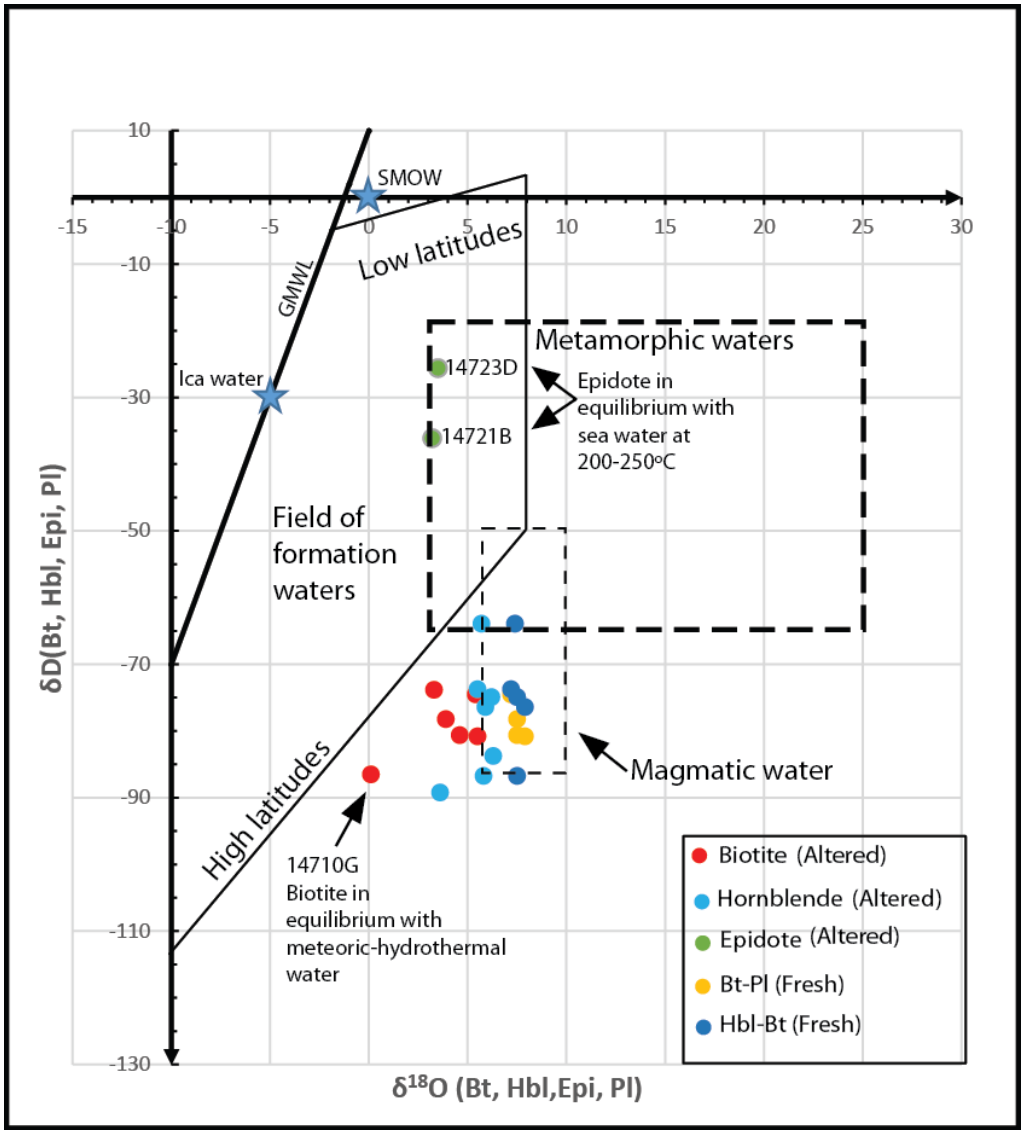

Figure 8. The δD and δ18O values of biotite (Bt), hornblende (Hbl), plagioclase (Pl) and epidote (Epi), for fresh and altered samples with respect to different water sources (Rollinson, 1993).

Table 2. Values for the B coefficient in equation (2), according to Bottinga and Javoy (1975) using quartz as the standard. b = mole fraction of anorthite in the feldspar. (The value for plagioclase we are using in our calculations). Blue color means an estimated value for epidote (Park and Ripley, 1999). Since quartz is the standard, its value is set to zero in the third column.*

Mineral	(Bottinga and Javoy, 1975) $B_{mineral}$	$B_{mineral}$-B_{quartz}
Quartz	–1.594	0
Feldspar	1.04(b – 0.6)	
If…		
anorthite = 0%	1.04(0 – 0.6)	0.97
anorthite = 35%	1.04(0.35-0.6)	1.33*
anorthite = 50%	1.04(0.5-0.6)	1.49
anorthite = 100%	1.04(1-0.6)	2.01
Amphibole	1.554	3.15
Actinolite	1.754	3.348
Biotite	2.096	3.69
Epidote		5
Magnetite	3.976	5.57

Isotopic values of meteoric water are governed by the Global Meteoric Water Line (GMWL) equation (Faure and Mensing, 2009; Yeh et al., 2014) whose mathematical expression is equation (3).

$$\delta D = 8\delta^{18}O + 10 \quad (3)$$

The values of δD and $\delta^{18}O$ displayed by meteoric water are a function of geographic location, becoming increasingly lighter going from the equator to the poles and from coastal to inland areas (Bowen and Revenaugh, 2003; Ohmoto, 1986; Sharp, 2007).

Meteoric water in the Ica-Pisco section of the PCB has an average $\delta^{18}O$ value of approximately –5‰ (Bowen and Revenaugh, 2003). Thus, according to equation (3), δD would be –30‰, assuming that these waters follow the Global Meteoric Water Line trend. However, the interaction of this low $\delta^{18}O$ meteoric water with plutonic intrusions in subduction environments causes an increase in water temperature (Ohmoto, 1996; Pirajno, 2009; Sharp, 2007; Taylor, 1979; Turi, 1988), which brings about a depletion of ^{18}O in both the pluton and the country rock and a corresponding ^{18}O enrichment or a "^{18}O shift" in the meteoric water. This process causes plutonic rock to have very low and even negative values for $\delta^{18}O$ (Criss and Taylor, 1986; Taylor, 1978; Turi, 1988).

6.2.2 *Water/rock ratio and intensity of fluid-rock interaction*

When magmas are intruded into the shallow crust, crystallize, and cool, they work as gigantic "heat engines" that produce the energy necessary to support a long-lasting convective circulation system of any H_2O in the country rocks. These waters are most commonly meteoric-hydrothermal water, if magmas were emplaced into a shallow crust subaerial environment (Criss and Taylor, 1986; Dilles et al., 1992; Brandriss et al., 1995) and seawater for a submarine system (Gregory and Taylor, 1981; Cathles, 1993; Holk et al., 2008). This interaction changes $\delta^{18}O$ and δD values of both water and rock (e.g., Taylor, 1974). Nevertheless, unaltered igneous rocks have a definite range of isotopic values (Bindeman, 2008; Rollinson, 1993; Sharp, 2007) that can be used for comparison to determine the effects of any processes that considerably alter their $\delta^{18}O$ values (Taylor, 1974).

Oxygen isotope ratios of hydrothermally altered igneous rocks are useful data for determining the amount of water that has interacted with the rock (Larson and Zimmerman, 1991; Taylor, 1977). A first estimate of the amount of water involved in a closed meteoric hydrothermal system can be determined by the material balance equation (Gregory et al., 1989; Taylor, 1974),

$$W\delta^{i}_{H_2O} + R\delta^{i}_{rock} = W\delta^{f}_{H_2O} + R\delta^{f}_{rock} \quad (4)$$

where i = initial $\delta^{18}O$ value, f = final $\delta^{18}O$ value after reaction, W = atom percent of meteoric water oxygen in the whole system and R = atom percent of rock oxygen in the total system. The water/rock ratio can be calculated by rearranging equation (4) to the form

$$\frac{W}{R} = \frac{\delta^{f}_{rock} - \delta^{i}_{rock}}{W\delta^{i}_{H_2O} - (\delta^{i}_{rock} - \Delta)} \quad (5)$$

where $\Delta = \delta^{f}_{rock} - \delta^{f}_{H_2O}$ given by the application of the $^{18}O/^{16}O$ fractionation factor for the temperature of hydrothermal activity.

Values of $\delta^{18}O$ for fresh and altered samples are compared in Table 3, where equation (5) was used to estimate the water/rock ratio involved in the alteration.

Equation (5) was also used to determine the magnitude of change undergone by the $\delta^{18}O$ values of fresh samples during the alteration process as well as the type of fluid that probably caused the alteration.

7. DISCUSSION

To better understand the discussion below, it is important to remember that $\delta^{18}O$ values of coexisting minerals in isotopic equilibrium in unaltered granitic rocks, increase in the following order: magnetite-biotite-amphibole-muscovite-plagioclase-K-feldspar-quartz (Taylor, 1978) showing a general increase in $\delta^{18}O$ values with increasing wt% SiO_2. The relative values with respect to quartz for the minerals mentioned above as suggested by Bottinga and Javoy (1975) are summarized in Table 2. Park and Ripley (1999) suggest an estimated value of 5 for epidote in Table 2.

7.1 *Classification of fresh samples based on their $\delta^{18}O$ values*

Based on their whole rock $\delta^{18}O$ values, plutonic rocks can be classified into three types (Taylor, 1978): a) low $\delta^{18}O$ granitic rocks with $\delta^{18}O$ < +6‰, b) normal $\delta^{18}O$ granitic rocks with +6‰ < $\delta^{18}O$ < +10‰, and c) high $\delta^{18}O$ granitic rocks with $\delta^{18}O$ > +10‰. Since plagioclase is the most abundant mineral in igneous rocks, $\delta^{18}O$ values of plagioclase are the closest to the whole rock $\delta^{18}O$ value and would be considered representative, if the rock is demonstrated to be in $^{18}O/^{16}O$ equilibrium. Using the criteria above, it is clear that all $\delta^{18}O$ values for fresh samples in Table 1 that demonstrate equilibrium and escaped subsolidus hydrothermal alteration are in the normal range for granitic rocks.

The normal range of hydrogen isotope values for granitic rocks is –85‰ < δD < –50‰ (Taylor, 1978). A plot of biotite and hornblende δD values vs plagioclase $\delta^{18}O$ values (Figure 8) shows that most of these samples lie within the rectangular area labeled as the primary magmatic zone of Taylor (1974), consistent with the fresh condition of these rocks.

7.2 *$\delta^{18}O$ values of altered samples*

Hydrothermal alteration is a complex process involving mineralogical, chemical, isotopic, and textural changes caused by the interaction of hydrothermal fluids that circulate through rocks under variable and changing physiochemical conditions (e.g., Pirajno, 2009; Rose and Burt, 1979).

The circulation of hydrothermal fluids is greatly accelerated by faults whose occurrence enhances permeability (Fetter, 2001; Hartman et al., 2018). Joints and faults provide conduits that allow hydrothermal fluids to quickly migrate until they cool and precipitate their mineral content or react with and replace dissolvable country rocks, a process able to produce a variety of alteration types (Guilbert and Park, 1986). In accordance with the previous statements, Agar (1981) mentions that hydrothermal alteration observed in the Ica-Pisco section is associated with the circulation of hydrothermal fluids along faults. Figure 9 shows some of the faults in the Ica-Pisco section as well as the areas affected by different types of alteration.

Unit	Sample	$\delta^{18}O$ (‰) 1 2 3 4 5 6 7 8 9 10	W/R	Type of fluid
Pampahuasi	14716G	7.2 → 9.3	0.2	Metamorphic
Pampahuasi	14723D	6.8 ← 7.2	0.05	Meteoric-magmatic
Pampahuasi	14725F	6.9 ← 7.2	0.04	Meteoric-magmatic
Pampahuasi	14723Aa	7.2 → 8.4	0.1	Metamorphic
Rinconada	14724Ac	5.7 ← 7.5	0.3	Meteoric?
Auquish	14721B	7.1 ← 7.5	0.05	Meteoric-magmatic
Auquish	14721Ac	5.5 ← 7.5	0.3	Meteoric?
Humay	14714Ca	6.7 → 7.6	0.08	Metamorphic
Humay	14714Eb	6.7 → 8.2	0.1	Metamorphic
Quilmana	14714Cb	7.4 ← 7.6	0.03	Meteoric-magmatic
Yura Group	14710G	2.6 ← 7.5	1.6	Meteoric

Table 3. δ18O values for plagioclase in altered samples with respect to fresh samples, displaying direction and magnitude of the alteration, probable fluid involved, and water/rock ratio calculated using equation (5) in the text.

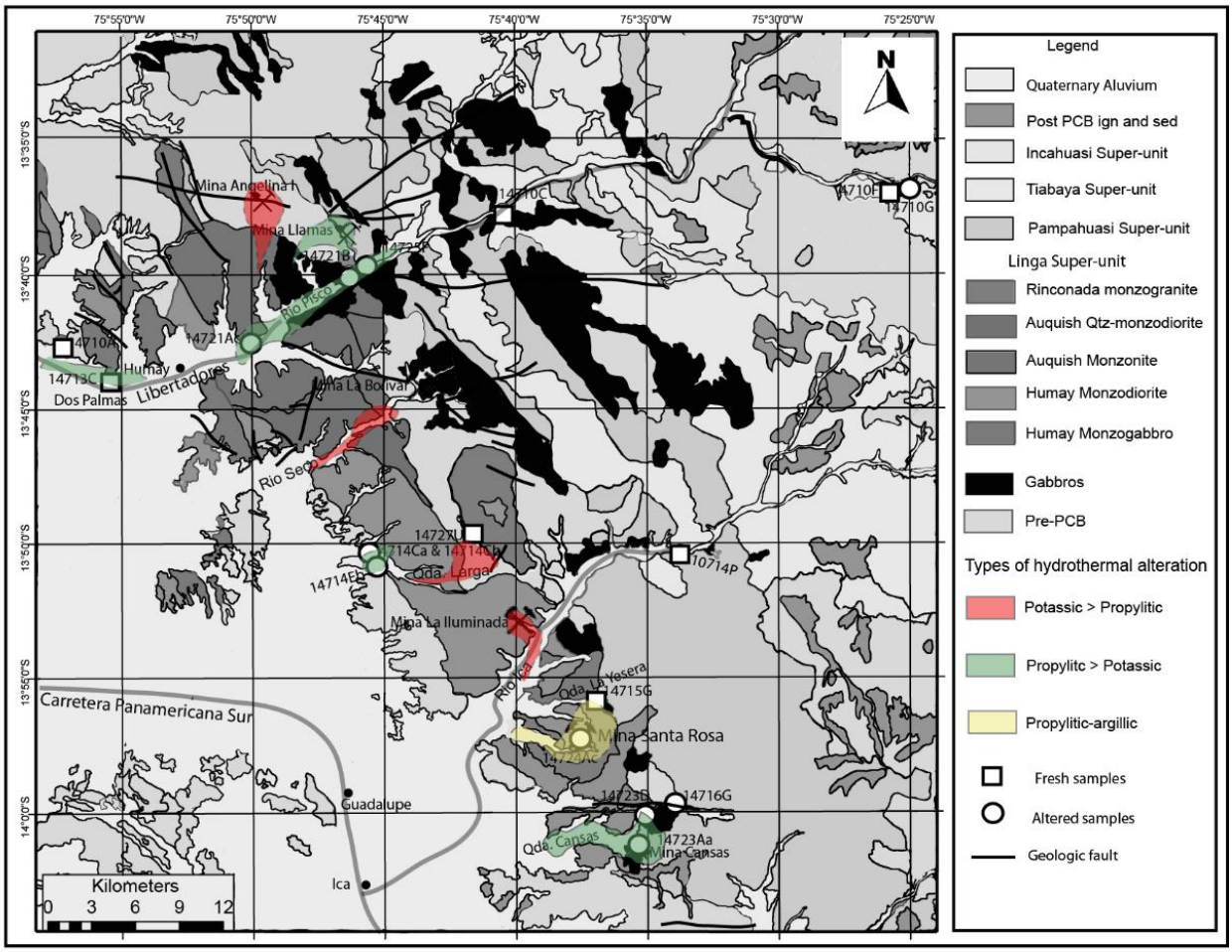

Figure 9. Approximate areal extent of the different types of hydrothermal alteration observed in the Linga complex. Quadrangles 28-i (Guadalupe) and parts of quadrangles 20-m (Santiago de Chocorvos), 29-m (Cordova) and 29-i (Ica). Adapted from Instituto Geológico, Minero y Metalúrgico del Perú (INGEMMET, 1978).

Table 1 shows the δD and $\delta^{18}O$ values for the 11 altered samples. Note that 5 out of 7 $\delta^{18}O$ plagioclase values from altered samples belong to the normal range proposed by Taylor (1978). This suggests that the alteration of most samples was caused by hydrothermal fluid of magmatic origin (Sharp, 2007; Sheppard, 1986).

Altered samples whose plagioclase $\delta^{18}O$ show values below those in equilibrium with magmatic fluids are from the Yura volcanics (14710G, $\delta^{18}O$ = +2.6‰), the Linga-Auquish (14721Ac, $\delta^{18}O$ = +5.5‰), and a sample associated with copper mineralization (14724Ac, $\delta^{18}O$ = +5.7‰). These $\delta^{18}O$ values are probably due to $^{18}O/^{16}O$ exchange with heated meteoric-hydrothermal water (Sharp, 2007; Taylor, 1978).

According to Table 3, the lowest water/rock ratio involved in the change of $\delta^{18}O$ values is 0.03. This value belongs to the Quilmana volcanics sample 14714Cb whose variation is from +7.6‰ to +7.4‰. Since this is a decrease from the original value, the change may just be due to the margin of error in measurement (a 3% error introduces error bars of ±0.2‰ in the calculations), but could also be caused by a very small contribution of meteoric water. However, the decrease from +7.6‰ to +7.4‰ still remains in the interval of magmatic fluids, which suggests that the main interaction was with magmatic hydrothermal fluids.

The biggest increase in $\delta^{18}O$ values from +7.2‰ to +9.3‰ belongs to sample 14716G from the metamorphic aureole where the Pampahuasi intrudes the Quilmana volcanics in the Rio Cansas transect. The water/rock ratio of 0.2 in Table 3 suggests that the increase may have resulted from the interaction of 1part external metamorphic fluids with 5 parts rock or magmatic fluids. In fact the $\delta^{18}O$ value for this altered sample is in the range of magmatic hydrothermal fluids.

The biggest decrease in $\delta^{18}O$ values in Table 3 is from +7.5‰ to +2.6‰ and belongs to sample 14710G from the Yura group. The direction of the isotopic change as well as the high water/rock ratio of 1.6 suggest that large amounts of meteoric fluids may have been involved in the alteration. The dominance of meteoric hydrothermal fluids interacting with this sample is supported by the low $\delta^{18}O$ value of biotite +0.1%. The depletion in ^{18}O value in this sample, agrees with the effect of magmatic intrusions heating water, bringing about a ^{18}O enrichment of water and causing plutonic rock to reach very low and even negative values for $\delta^{18}O$.

7.3 *δD for fresh and altered samples*

Hydrothermal fluids are a major source of various components of hydrothermal ore deposits formed in volcanic arcs. These components, including metals and their ligands, become concentrated in magmas in various ways from various sources, including subducted oceanic crust and leaching of rocks (Hedenquist and Lowenstern, 1994). Thus, the fact that most of the samples in Table 1, either fresh or altered, have δD values in the normal isotopic range for plutonic rocks, i.e. –85‰ < δD < –50‰, can be explained by noting that most primary magmatic water may have originated from OH^--bearing minerals (clays, micas, amphiboles) of subducted sediments and altered volcanic rocks that have been introduced into the lower crust or the upper mantle through geologic time. These subducted materials are directly melted or dehydrated at high temperatures in the upper mantle, and the resulting hydrothermal fluid is incorporated into the calc-alkaline magmas produced in subduction-zone environments, like those producing the Linga complex of the PCB (Burnham, 1979; Hoefs, 1996; Stakes, 1991; Taylor, 1979; Wilson, 1989). Nevertheless, the high δD –25.6‰ epidote value of sample 14723D and –36‰ for sample 14721B do not fit in the normal interval for δD values of Taylor (1974). These values could be the result of interaction between the rock and seawater probably infiltrating the western side of the batholith.

8. CONCLUSIONS

An oxygen isotope closure temperature of 590°C to 650°C recorded for unaltered samples indicates the preservation of magmatic values and any fluids related to such rocks were magmatic in origin. The slight increase in $\delta^{18}O$ values of fresh samples from west to east and as ages get younger suggests an increased crustal contribution to these magmas with time and distance away from the continental margin.

Potassic (~ 450-600°C) and propylitic alteration (~ 250-350°C) dominates the center, and southeast and northwest extremes of the Linga complex, respectively. Phyllic (~ 200-350°C) and argillic alteration (~ 100-200°C) are present, but not as abundant in the Linga complex as the previously mentioned alteration types. Oxygen and hydrogen isotope data indicate that magmatic fluids were responsible for this alteration, but evidence is provided for limited involvement of meteoric-hydrothermal, metamorphic, and seawater fluids at small water/rock ratio.

ACKNOWLEDGMENTS

This research was supported by the Geoscience Research Institute, the Department of Earth and Biological Sciences at Loma Linda University, Montemorelos University, NSF-EAR grant 0949044, and the California State University, Long Beach Office of Research and Scholarly Activities. We thank Juan Carlos Molano for discussions, as well as Ana Martinez, Lance Pompe and Ed Santos for valuable support in field work and mapping. We also thank Mr.Teodosio Ramos, the owner of Ramos Minerals S. R, in Lima, Peru, for sharing mining information.

REFERENCES

Agar, R. A., 1978, The Peruvian Coastal Batholith: Its Monzonitic Rocks and their Related Mineralization [Doctor of Philosophy]: University of Liverpool, 293 p.

-, 1981, Copper mineralization and magmatic hydrothermal brines in the Rio Pisco section of the Peruvian Coastal Batholith: Economic Geology, v. 76, p. 677-693.

Agar, R. A., and Le Bel, L., 1985, The Linga Super-unit: High-K diorites of the Arequipa segment, *in* W.S. Pitcher, M. P. Atherton, Cobbing, E. J., and Beckinsale, R. D., eds., Magmatism at a Plate Edge: The Peruvian Andes: New York, John Wiley and Sons., p. 119-127.

Aguirre, L., and Offler, R., 1985, Burial metamorphism in the Western Peruvian Trough: its relation to Andean magmatism and tectonics, *in* W.S. Pitcher, M. P. Atherton, Cobbing, E. J., and Beckinsale, R. D., eds., Magmatism at a plate edge: The Peruvian Andes: New York, John Wiley and Sons, p. 59-71.

Atwater, T., 1970, Implications of plate tectonics for the Cenozoic tectonic evolution of western North America: GSA Bulletin, v. 81, no. 12, p. 3513-3536.

Barnes, I., 1970, Metamorphic waters from the Pacific Tectonic Belt of the West Coast of the United States: Science, v. 168, no. 3934, p. 973-975.

Beckinsale, R. D., Sanchez-Fernandez, A. W., Brook, M., Cobbing, E. J., Taylor, W. P., and Moore, N. D., 1985, Rb-Sr whole rock isochron and K-Ar age determinations for the Coastal Batholith of Peru, *in* W.S. Pitcher, M. P. Atherton, Cobbing, E. J., and Beckinsale, R. D., eds., Magmatism at a plate edge: The Peruvian Andes: New York, John Wiley and Sons, p. 177-202.

Bindeman, I., 2008, Oxygen isotopes in mantle and crustal magmas as revealed by single crystal analysis: Reviews in Mineralogy and Geochemistry, v. 69, p. 445-478.

Boekhout, F., Sempere, T., Spikings, R., and Schaltegger, U., 2013, Late Paleozoic to Jurassic chronostratigraphy of coastal southern Peru: Temporal evolution of sedimentation along an active margin: Journal of South American Earth Sciences, v. 47, p. 179-200.

Bottinga, Y., and Javoy, M., 1975, Oxygen isotope partitioning among the minerals in igneous and metamorphic rocks: Reviews of Geophysics and Space Physics, v. 13, no. 2, p. 401-418.

Bowen, G. J., and Revenaugh, J., 2003, Interpolating the isotopic composition of modern meteoric precipitation: Water Resources Research, v. 39, no. 10, 1299, p. 1-13.

Brandriss, M. E., Nevle, R. J., Bird, D. K., and O'Neil, J. R., 1995, Imprint of meteoric water on the stable isotope compositions of igneous and secondary minerals, Kap Edvard Holm Complex, East Greenland: Contributions to Mineralogy and Petrology, v. 12, no. 1, p. 74-86.

Burnham, C. W., 1979, Magmas and hydrothermal fluids, *in* Barnes, H. L., ed., Geochemistry of Hydrothermal Ore Deposits: New York, John Wiley & Sons, p. 71-136.

Cathles, L.M., 1993, Oxygen isotope alteration in the Noranda mining district, Abitibi greenstone belt, Quebec: Economic Geology, v. 88, p. 1483-1511.

Clausen, B. L., Morton, D. M., Kistler, R. W., and Lee, C. A., 2014, Low-initial-Sr felsic plutons of the northwestern Peninsular Ranges batholith, southern California, and the role of mafic-felsic magma mixing in continental crust formation, *in* Morton, D. M., and Miller, F. K., eds., Peninsular Ranges Batholith, Baja California and Southern California: USA, GSA Memoir 211, p. 317-344.

Cobbing, E. J., and Pitcher, W. S., 1972, The Coastal Batholith of Central Peru: Geological Society of London Journal, v. 128, no. 5, p. 421-460.

Cobbing, E. J., Pitcher, W. S., and Taylor, W. P., 1977, Segments and Super-units in the Coastal Batholith of Peru: Journal of Geology, v. 85, no. 5, p. 625-631.

Criss, R. E., and Taylor, H. P., 1986, Meteoric hydrothermal systems: Reviews in Mineralogy and Geochemistry, v. 16, no. 1, p. 373-424.

Damian, F., 2003, The mineralogical characteristics and the zoning of the hydrothermal types alteration from nistru ore deposit, Baia Mare metallogenetic district: Geologia, v. XLVIII, no. I, p. 101-112.

De Haller, A., Corfu, F., Urs, L. F., Barra, F., Chiaradia, M., Frank, M., and Julio, Z., 2006, Geology, geochronology, and Hf and Pb isotope data of the Raúl-Condestable iron oxide-copper-gold deposit, Central Coast of Peru: Economic Geology, v. 101, no. 2, p. 281-310.

DePaolo, D. J., 1981, Trace element and isotopic effects of combined wallrock assimilation and fractional crystallization: Earth and Planetary Science Letters, v. 53, p. 189-202.

Dilles, J. H., Solomon, G. C., Taylor, H. P., and Einaudi, M. T., 1992, Oxygen and hydrogen isotope characteristics of hydrothermal alteration at the Ann-Mason Porphyry Copper Deposit, Yerington, Nevada: Economic Geology, v. 87, p. 44-63.

Faure, G., 1998, Principles and Applications of Geochemistry, USA, Prentice Hall.

Faure, G., and Mensing, T. M., 2009, Isotopes, Principles and Applications, Delhi, Wiley India Pvt. Ltd.

Fetter, C. W., 2001, Applied Hydrogeology, USA, Prentice-Hall.

Garcia, M. O., Ito, E., and Eiler, A. M., 2008, Oxygen isotope evidence for chemical interaction of Kilauea historical magmas with basement rocks: Journal of Petrology, v. 49, no. 4, p. 757-769.

German, C. R., and Lin, J., 2004, The thermal structure of the oceanic crust, ridge-spreading and hydrothermal circulation: How well do we understand their inter-connections?, *in* German, C. R., Lin, J., and Parson, L. M., eds., Mid-Ocean Ridges, Volume 148, p. 1-18.

Giachetti, T., Gonnermann, H. M., Gardner, J. E., Shea, T., and Gouldstone, A., 2015, Discriminating secondary from magmatic water in rhyolitic matrix-glass of volcanic pyroclasts using thermogravimetric analysis: Geochimica et Cosmochimica Acta, v. 148, p. 457-476.

Giletti, B. J., and Hess, K. C., 1988, Oxygen diffusion in magnetite: Earth and Planetary Science Letters, v. 89, no. 1, p. 115-122.

Gregory, R. T., and Criss, R. E., 1986, Isotopic exchange in open and closed systems, *in* Valley, J. W., Taylor H P, J., and O'Neil, J. R., eds., Reviews in Mineralogy, Volume 16: USA, p. 91-127.

Gregory, R. T., Criss, R. E., and Taylor, H. P., 1989, Oxygen isotope exchange kinetics of mineral pairs in closed and open systems: applications to problems of hydrothermal alteration of igneous rocks and Precambrian iron formations: Chemical Geology, v. 75, no. 1-2, p. 1-42.

Gregory R.T., and Taylor, H.P., Jr., 1981, An oxygen isotope profile in a section of Cretaceous oceanic crust, Samial ophiolite, Oman: evidence for $\delta^{18}O$ buffering of the oceans by deep (> 5 km) seawater-hydrothermal circulation at mid-ocean ridges: Journal of Geophysical Research, v. 86, p. 2737-2755.

Grunder, A. L., 1992, Two-stage contamination during crustal assimilation: isotopic evidence from volcanic rocks in eastern Nevada: Contributions to Mineralogy and Petrology, v. 112, no. 2-3, p. 219-229.

Guilbert, J. M., and Park, C. F., 1986, The Geology of Ore Deposits, USA, W. H. Freeman and Company.

Harris, A. C., and Golding, S. D., 2002, New evidence of magmatic-fluid–related phyllic alteration: Implications for the genesis of porphyry Cu deposits: Geology, v. 30, no. 4, p. 335-338.

Harris, C., and Chaumba, J., 2001, Crustal contamination and fluid-rock interaction during the formation of the Platreef, northern limb of the Bushveld complex, South Africa: Journal of Petrology, v. 42, no. 7, p. 1321-1347.

Hartman, S.M., Paterson, S.R., Holk, G.J., and Kirkpatrick, J., 2018, Structural and hydrothermal evolution of a strike-slip shear zone during a ductile-brittle transition, Sierra Nevada, CA: Journal of Structural Geology (*in press)*.

Hedenquist, J. W., Arribas, A., and Gonzalez, E., 2000, Exploration for epithermal gold deposits: SEG reviews, v. 13, p. 245-277.

Hedenquist, J. W., and Lowenstern, J. B., 1994, The role of magmas in the formation of ore deposits: Nature, v. 370, p. 519-527.

Hoefs, J., 1996, Stable Isotope Geochemistry, Germany, Springer.

Holk, G.J., Taylor, B.E., and Galley, A.G., 2008, Oxygen isotope mapping of the Archean Sturgeon Lake caldera complex and VMS-related hydrothermal system, northwestern Ontario, Canada: Mineralium Deposita, v. 43, p. 623-640.

Holk, G. J., Grove, M., Jacobson, C. E., and Haxel, G. B., 2016, A two-stage fluid history for the Orocopia Schist and associated rocks related to flat subduction and exhumation, southeastern California: International Geology Review, v. 59, no. 5-6, p. 639-663.

Humphris, S. E., 1976, The Hydrothermal Alteration of Oceanic Basalts by Seawater [Doctor of Philosophy: Massachusetts Institute of Technology, 248 p.

Husband, M. E., 1998, Modeling the Mobilization of Connate Water while Injecting Water to Displace Oil [Doctor of Philosophy]: Texas Tech University, 202 p.

INGEMMET, 1978, Quadrangle 28-i (Guadalupe), and parts of quadrangles 28-m (Santiago de Chocorvos) , 29-m (Cordova), and 29-i (Ica): Perú, Sector energía y minas del Perú.

Jaillard, E., and Soler, P., 1996, Cretaceous to early Paleogene tectonic evolution of the northern Central Andes (0-18^{o}S) and its relations to geodynamics: Tectonophysics, v. 259, p. 41-53.

Javoy, M., 1977, Stable isotopes and geothermometry: Journal of the Geological Society, v. 133, no. 6, p. 609-636.

Javoy, M., Fourcade, S., and Allegre, C. J., 1970, Graphical method for examination of $^{18}O/^{16}O$ fractionations in silicate rocks: Earth and Planetary Science Letters, v. 10, p. 12-16.

Jebrak, M., 1997, Hydrothennal breccias in vein-type ore deposits: A review of mechanisms, morphology and size distribution: Ore Geology Reviews, v. 12, p. 111-134.

Johnson, K. E., Harmon, R. S., Richardson, J. M., Moorbath, S., and Strong, D. F., 1996, Isotope and trace element geochemistry of Augustine Volcano, Alaska: Implications for magmatic evolution: Journal of Petrology, v. 37, no. 1, p. 95-115.

Langenheim, V. E., Jachens, R. E., Morton, D. M., Kistler, R. W., and Matti, J. C., 2004, Geophysical and isotopic mapping of preexisting crustal structures that influenced the location and development of the San Jacinto fault zone, southern California: GSA Bulletin, v. 116, no. 9-10, p. 1143-1157.

Larson, P. B., and Zimmerman, B. S., 1991, Variations in $\delta^{18}O$ values, water/rock ratios, and water flux in the Rico paleothermal anomaly, Colorado: The Geochemical Society, Special Publication, v. 3, p. 463-469.

Le Bel, L. M., 1985, Mineralization in the Arequipa segment: The porphyry-Cu deposit of Cerro Verde/Santa Rosa, *in* W.S. Pitcher, M. P. Atherton, Cobbing, E. J., and Beckinsale, R. D., eds., Magmatism at a plate edge: The Peruvian Andes: New York, John Wiley and Sons, p. 250-260.

Markl, G., and Baumgartner, L., 2002, pH changes in peralkaline late-magmatic fluids: Contributions to Mineralogy and Petrology, v. 144, no. 3, p. 331-346.

Martinez, A. M., 2016, Compositional Diversity in Arcs: A Record of Magmatic Processes in the Peru Coastal Batholith, Ica. [Doctor of Philosophy]: Loma Linda University, 410 p.

Martinod, J., Husson, L., Roperch, P., Guillaume, B., and Espurt, N., 2010, Horizontal subduction zones, convergence velocity and the building of the Andes: Earth and Planetary Science Letters, v. 299, p. 299-309.

McQuarrie, N., Horton, B., K, Zandt, G., Beck, S., and DeCelles, P., G., 2005, Lithospheric evolution of the Andean fold-thrust belt, Bolivia, and the origin of the central Andean plateau: Tectonophysics v. 399, p. 15-37.

Mégard, F., 1984, The Andean orogenic period and its major structures in central and northern Peru: Journal of the Geological Society, v. 141, no. 5, p. 893-900.

Meunier, A., and Velde, B., 2004, Illite: Origins, Evolution and Metamorphism, Germany, Springer.

Moore, N. D., 1979, The Geology and Geochronology of the Arequipa Segment of the Coastal Batholith of Peru [Doctor in Philosophy]: Liverpool, 549 p.

-, 1984, Potassium-argon ages from the Arequipa segment of the Coastal Batholith of Peru and their correlation with regional tectonic events: Journal of the Geological Society, v. 141, no. 3, p. 511-519.

Mukasa, S. B., 1986, Zircon U-Pb ages of Super-units in the Coastal Batholith, Peru: Implications for magmatic and tectonic processes: GSA Bulletin, v. 97, p. 241-254.

Mysen, B., 2014, Water-melt interaction in hydrous magmatic systems at high temperature and pressure: Progress in Earth and Planetary Science, v. 1, no. 1, p. 1-18.

Ohmoto, H., 1986, Stable isotope geochemistry of ore deposits: Reviews in Mineralogy and Geochemistry, v. 16, no. 1, p. 491-559.

-, 1996, Formation of volcanogenic massive sulfide deposits: The Kuroko perspective: Ore Geology Reviews, v. 10, p. 135-177.

Park, Y.-R., and Ripley, E. M., 1999, Hydrothermal flow systems in the Midcontinent Rift: Oxygen and hydrogen isotopic studies of the North Shore Volcanic Group and related hypabyssal sills, Minnesota: Geochimica et Cosmochimica Acta, v. 63, no. 11-12, p. 1787-1804.

Pfiffner, O. A., and Gonzalez, L., 2013, Mesozoic–Cenozoic evolution of the western margin of South America: Case study of the Peruvian Andes: Geosciences, v. 3, p. 262-310.

Pirajno, F., 2009, Hydrothermal Processes and Mineral Systems, Australia, Springer.

Plank , T., Kelley , K. A., Zimmer , M. M., Hauri , E. H., and Wallace, P. J., 2013, Why do mafic arc magmas contain ~4 wt% water on average?: Earth and Planetary Science Letters, v. 364, p. 168-179.

Polliand, M., Schaltegger, U., Frank, M., and Fontbote, L., 2005, Formation of intra-arc volcanosedimentary basins in the western flank of the central Peruvian Andes during Late Cretaceous oblique subduction: field evidence and constraints from U-Pb ages and Hf isotopes: International Journal of Earth Sciences, v. 94, no. 2, p. 231-242.

Que, M., and Allen, A. R., 1996, Sericitization of plagioclase in the Rosses Granite Complex, Co. Donegal, Ireland: Mineralogical Magazine, v. 60, p. 927-936.

Ripley, E. M., and Ohmoto, H., 1979, Oxygen and hydrogen isotopic studies of ore deposition and metamorphism at the Raul mine, Peru: Geochimica and Cosmochimica Acta, v. 43, p. 1633-1643.

Robb, L., 2005, Introduction to ore-forming processes, Victoria, Australia, Blackwell Science Ltd.

Rohling, E. J., 2013, Oxygen isotope composition of seawater, *in* Elias, S. A., ed., The Encyclopedia of Quaternary Science, Volume 2: Amsterdan, Elsevier, p. 915-922.

Rollinson, H. R., 1993, Using Geochemical Data: Evaluation, Presentation, Interpretation, UK, Pearson Prentice-Hall.

Rose, A. W., and Burt, D. M., 1979, Hydrothermal alteration, *in* Barnes, H. L., ed., Geochemistry of Hydrothermal Ore Deposits: New York, John Wiley & Sons, p. 173-227.

Rutherford, M. J., and Devine, J. D., 2003, Magmatic conditions and magma ascent as indicated by hornblende phase equilibria and reactions in the 1995-2002 Soufriere Hills magma: Journal of Petrology, v. 44, no. 8, p. 1433-1454.

Santo, A. P., and Peccerillo, A., 2008, Oxygen isotopic variations in the clinopyroxene from the Filicudi volcanic rocks (Aeolian Islands, Italy): Implications for open-system magma evolution: The Open Mineralogy Journal, v. 2, p. 22-33.

Schilling, F. R., Trumbull, R. B., Brasse, H., Haberland, C., Asch, G., Bruhn, D., Mai, K., Haak, V., Giese, P., Muñoz, M., Ramelow, J., Rietbrock, A., Ricaldi, E., and Vietor, T., 2006, Partial melting in the Central Andean crust: A

review of geophysical, petrophysical, and petrologic evidence, *in* Oncken, O., Chong, G., Franz, G., Giese, P., Götze, H. J., Ramos, V. A., Strecker, M. R., and Wigger, P., eds., The Andes: Berlin, Springer, p. 459-474.

Schmidt, K. L., and Paterson, S. R., 2002, A doubly vergent fan structure in the Peninsular Ranges batholith: Transpression or local complex flow around a continental margin buttress?: Tectonics, v. 21, no. 5, p. 1-19.

Schweickert, R. A., and Cowan, D. S., 1975, Early Mesozoic tectonic evolution of the western Sierra Nevada, California: GSA Bulletin, v. 86, no. 10, p. 1329-1336.

Seyfried, W. E., Berndt, M. E., and Seewald, J. S., 1988, Hydrothermal alteration processes at mid-ocean ridges: Constraints from diabase alteration experiments hot-spring fluids and composition of the oceanic crust: Canadian Mineralogist, v. 26, p. 787-804.

Sharp, Z. D., 1990, A laser-based microanalytical method for the in situ determination of oxygen isotope ratios of silicates and oxides: Geochimica et Cosmochimica Acta, v. 54, p. 1353-1357. 2007, Principles of Stable Isotope Geochemistry, USA, Pearson Prentice-Hall.

Sharp, Z. D., Atudorei, V., and Durakiewicz, T., 2001, A rapid method for determination of hydrogen and oxygen isotope ratios from water and hydrous minerals: Chemical Geology, v. 178, p. 197-210.

Sheppard, S. M. F., 1986, Characterization and isotopic variations in natural waters, *in* Valley, J. W., Taylor, H. P., and O'Neil, J. R., eds., Reviews in Mineralogy. Stable Isotopes in High Temperature Geological Processes, Volume 16: USA, Mineralogical Society of America, p. 165-183.

Silver, L. T., Taylor, H. P., and Chappell, B., 1979, Some petrological, geochemical and geochronological observations in the Peninsular Ranges batholith near the international border of the USA and Mexico, *in* Abbott, P. L., and Todd, B. R., eds., Mesozoic Crystalline Rocks: San Diego State University, Department of Geological Sciences, p. 83-110.

Soler, P., and Bonhomme, M. G., 1990, Relation of magmatic activìty to plate dynamics ìn central Peru from Late Cretaceous to present: GSA Special Paper, v. 241, p. 173-192.

Sparks, R. S. J., and Huppert, H. E., 1984, Density changes during the fractional crystallization of basaltic magmas: fluid dynamic implications: Contributions to Mineralogy and Petrology, v. 85, p. 300-309.

Springer, M., 1999, Interpretation of heat-flow density in the Central Andes: Tectonophysics, v. 306, no. 3,4, p. 377-395.

Stakes, D. S., 1991, Oxygen and hydrogen isotope compositions of oceanic plutonic rocks: High-temperature deformation and metamorphism of oceanic layer 3: The Geochemical Society, v. 3, p. 77-90.

Sykes, M. L., 1987, Evolution of granitic magmas during ascent: A phase equilibrium model: The Geochemical Society, Special Publication, v. 1, p. 447-462.

Taylor, B. E., 1986, Magmatic volatiles: Isotopic variation on C, H, and S, *in* Valley, J. W., Taylor H P, J., and O'Neil, J. R., eds., Stable Isotopes in High Temperature Geological Processes: USA, Mineralogical Society of America.

Taylor, H. P., 1974, The application of oxygen and hydrogen isotope studies to problems of hydrothermal alteration and ore deposition: Economic Geology, v. 69, p. 843-883.

1977, Water/rock interactions and the origin of H_2O in granitic batholiths: Thirtieth William Smith lecture: Journal of the Geological Society, v. 133, no. 6, p. 509-558.

1978, Oxygen and hydrogen isotope studies of plutonic granitic rocks: Earth and Planetary Science Letters, v. 38, no. 1, p. 177-210.

1979, Oxygen and hydrogen isotope relationships in hydrothermal mineral deposits, *in* Barnes, H. L., ed., Geochemistry of Hydrothermal Ore Deposits: New York, John Wiley & Sons, p. 236-277.

Taylor, H. P., and Sheppard, S. M. F., 1986, Igneous rocks: I. Processes of isotopic fractionation and isotope systematics, *in* Valley, J. W., Taylor, H. P., and O'Neil, J. R., eds., Reviews in Mineralogy. Stable Isotopes in High Temperature Geological Processes, Volume 16: USA, Mineralogical Society of America, p. 227-271.

Terzer, S., Wassenaar, L. I., Araguás, A. L. J., and Aggarwal, P. K., 2013, Global isoscapes for $d^{18}O$ and $d^{2}H$ in precipitation: Improved prediction using regionalized climatic regression models: Hydrology and Earth System Sciences, v. 17, p. 4713–4728.

Turi, B., 1988, Stable isotopes in petrology: a brief survey: Rendiconti della Societa Italiana di Mineralogia e Petrologia, v. 43, p. 83-94.

Wilson, M., 1989, Igneous Petrogenesis, The Netherlands, Springer.

Williams, H. M., Nielsen, S. G., Renac, C., Griffin, W. L., O'Reilly, S. Y., McCammon, C. A., Pearson, N. R., Viljoen, F., Alt, J. C., and Halliday, A. N., 2009, Fractionation of oxygen and iron isotopes by partial melting processes: Implications for the interpretation of stable isotope signatures in mafic rocks: Earth and Planetary Science Letters, v. 283, p. 156-166.

Winter, J. D., 2010, Principles of Igneous and Metamorphic Petrology, New Jersey, Prentice Hall.

Yardley, B. W. D., and Cleverley, J. S., 2013, The role of metamorphic fluids in the formation of ore deposits: Geological Society, London, Special Publications, v. 393, p. 1-18.

Yeh, H. F., Lin, H. I., Lee, C. H., Hsu, K. C., and Wu, C. S., 2014, Identifying seasonal groundwater recharge using environmental stable isotopes: Water, v. 6, p. 2849-2861.

Sociedad Geológica del Perú

SGP
FUNDADA 1924

Boletín Volumen 113

Órgano oficial de la Sociedad Geológica del Perú
Fundada el 3 de julio de 1924, en Lima

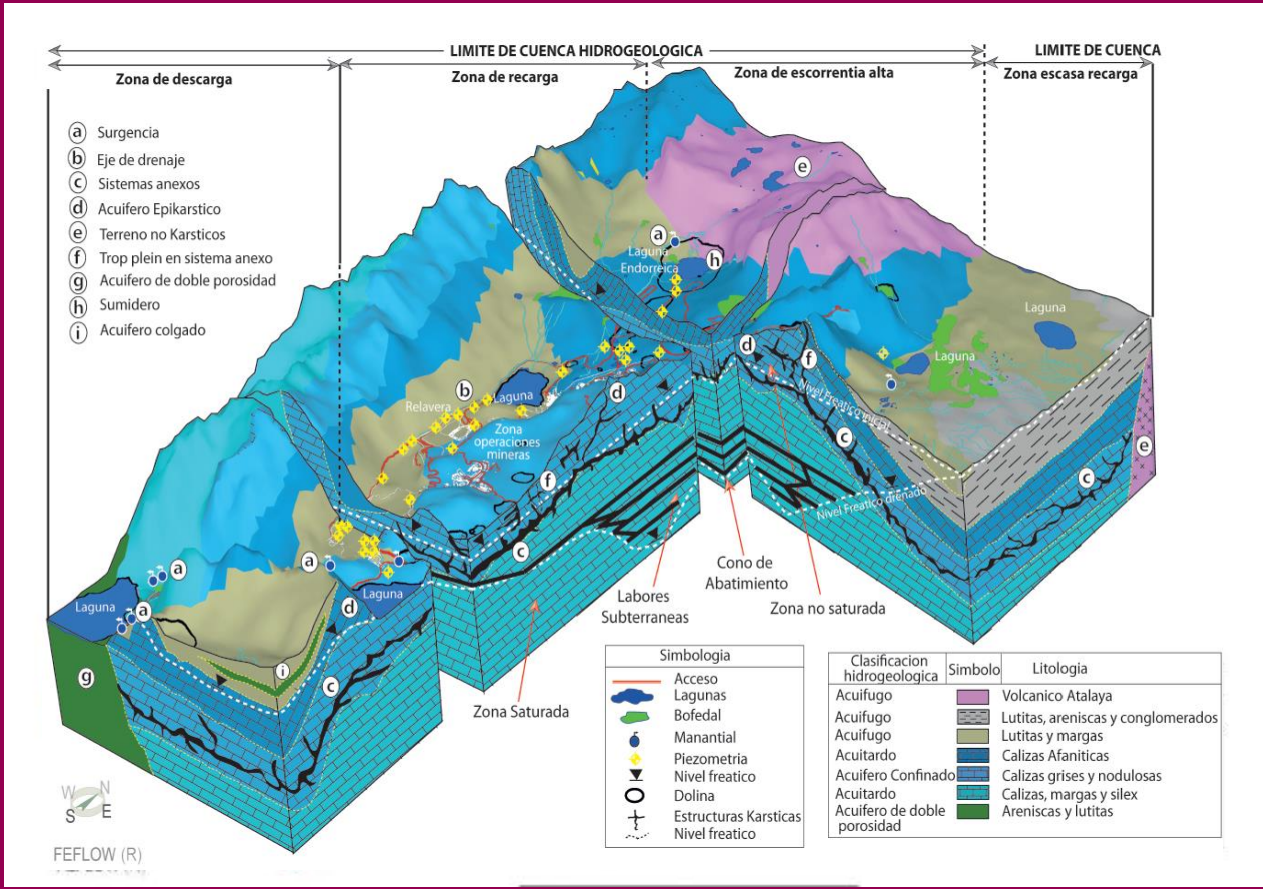

2020

ISSN: 0079 – 1091
Versión Digital.

Toda correspondencia relacionada con esta publicación
debe ser dirigida al editor responsable:
Sociedad Geológica del Perú, Av. 28 de Julio 745, Miraflores
Lima - Perú

Imágenes de portada:
Foto: *Modelo hidrogeológico del sistema kárstico de mina y sus singularidades. (Fuente; Mangin, 1975, Custodio Llamas 1976, Pulido Bosch 2014, modificado Hidroandes 2014)*

SOCIEDAD GEOLÓGICA DEL PERÚ

BOLETÍN DE LA SOCIEDAD GEOLÓGICA DEL PERÚ
Órgano oficial de la Sociedad Geológica del Perú fundada el 3 de julio de 1924, en Lima
Volumen editado durante el:

Sociedad Geológica del Perú
Teléfonos: (51-1) 628-1150 / 444-1180
Av. 28 de Julio 745 Miraflores - Lima 18 - Perú E-mail: sgp@sgp.org.pe - Web Site: www.sgp.org.pe

BOLETÍN DE LA SOCIEDAD GEOLÓGICA DEL PERÚ

Vol. 113

CONTENIDO

Percy Dimas, Edwin Mamani y Brenda Vilca 01
Estimación de la Recarga en Acuiferos Karsticos y su incidencia a una mina subterránea de Perú

Luciano Gonzáles, Benjamin Clausen, Gregory Holk y Orlando Poma 12
Using stable isotopes to better understand the petrologic and hydrothermal evolution of cretaceous Linga complex of the peruvian coastal batholith, near Ica

Fluquer Peña Laureano y Boris Santos Romero 26
El Humedal Costero Albuferas de Medio Mundo y su relación con el agua subterránea, Lima - Perú

Rubén Mamani, Marcelo Lavado, William Martinez y Yvan Mendoza 32
Geología Estructural de la mineralización del yacimiento aurífero Mishky región de Arequipa sur del Perú

Nestor Teves, Carmen San Román y Gustavo Laos 45
Vulnerabilidad costera en el Perú y el Calentamiento Global